Applied Radiation and Isotopes 115 (2016) 13–17

Contents lists available at ScienceDirect

Applied Radiation and Isotopes

journal homepage: www.elsevier.com/locate/apradiso

Remote radiation sensing module based on a silicon photomultiplier for industrial applications

Hye Min Park, Koan Sik Joo*

Department of Physics, University of Myongji, Yongin KS 009, Republic of Korea

HIGHLIGHTS

- We designed a SiPM based remote radiation sensing module for the radiation detection in a radioactive contamination zone.
- This system is powered by a Li-poly battery and it is small enough to be put in a pocket as a portable device for a worker.
- The Bluetooth capability of the SSRM provides a platform for continuous and remote monitoring of abnormal conditions.
- SiPM-based radiation detection technology could potentially be used for industrial applications.

ARTICLE INFO

Article history:
Received 20 March 2014
Received in revised form
2 June 2016
Accepted 2 June 2016
Available online 3 June 2016

Keywords:
Silicon photomultiplier (SiPM)
Bluetooth
Mcnpx

ABSTRACT

We have designed a silicon-photomultiplier-based remote radiation-sensing module consisting of a master port (displaying radiation information) and a slave port (detects radiation, transmits to master). The master port merges radiation and dose values and displays them. Counting detection efficiency and radiation response simulated using MCNPX were used to calibrate the module. We performed radioactive source tests (^{137}Cs, ^{22}Na, ^{60}Co, ^{55}Fe) and compared experimental and simulation results. Remote detection capability was demonstrated and the detection accuracy was determined. Applications abound in the radioactivity industry.

1. Introduction

The remote radiation sensing module (RRSM) is a device intended for industrial applications. The design goal for this device is to be a sensitive, portable, and real-time system for more accurate measurement of radiation and to improve the reliability of monitoring systems. Traditionally, the optical sensors of radiation monitoring system for industrial applications have been photomultiplier tubes (PMTs), avalanche photodiodes (APDs), or PIN silicon photodiodes (Table 1). However, these sensors have some limitations. The PMT requires a high voltage supply and leads to a bulky design of the instrument and an extensive sensitivity to magnetic fields. The APD requires a high voltage supply as well, but also stable temperatures in order to ensure the stability of the energy measurement. The use of PIN silicon photodiodes allows one to build compact probes without a high-voltage supply. The sensitivity to magnetic fields is low and the signal amplitude depends weakly on temperature changes. However, the PIN silicon photodiodes do not have the internal gain that APD and PMT have. Special attention must be paid in order to minimize electronic noise, which is higher than the statistical noise at low energies (Chavanelle and Parmentier, 2003).

On the other hand, a silicon photomultiplier (SiPM)-based device seems to be suitable for this system because of its physical superiority: its compact size, high gain, low voltage supply, and insensitivity to magnetic fields. Because of these properties, SiPM has been introduced in the field of radiation applications (Osovizky et al., 2011).

In this study, we focus on advancing the SiPM-based remote monitoring system for the purposes of distributed and environmental sensing in a radioactive contamination zone. This method of remote sensing has many potential benefits, primarily in environments for which leakage of radiation from equipment or facilities could potentially occur.

In the next section, we describe the fabrication of this platform. We then present the properties of the designed system in Section 3, followed by conclusions in Section 4.

* Corresponding author.
E-mail address: ramilab2011@gmail.com (K.S. Joo).

http://dx.doi.org/10.1016/j.apradiso.2016.06.002

2. Materials and methods

Our detection system uses a S12572-100C Hamamatsu multi-pixel photon counter (MPPC) with a photosensitive area of 3×3 mm^2 to minimize the overall system dimensions (Table 2). It was mounted on a CsI:Tl ($3 \times 3 \times 20$ mm^3) crystal. The CsI:Tl has a peak wavelength of around 550–570 nm, which fits the absorption spectral range of SiPM. Furthermore, with a density of 4.51 g cm^{-3}, it has good stopping power. The decay time (1 µs) was somewhat higher than that of the other considered scintillator, which would limit the count rate (Chavanelle and Parmentier., 2003). However, the light yield (52,000 photons/MeV) of this scintillator was very high. In order to maximize the light output from the CsI:Tl and match it to the SiPM photosensitive area, the crystal geometry was optimized using a Monte Carlo *n*-particle extended (MCNPX) code (Park and Joo, 2015). The radiation sources used in the simulation and the actual test were ^{137}Cs, ^{22}Na, ^{60}Co, and ^{55}Fe, each with an activity of 1 µCi.

For the functional verification of the composed system, we installed the designed module (slave port) in a radiation field, executed the radiation source tests and compared the results to those of the MCNPX code. The accuracy of the simulation was verified by implementation of the gamma ray dose constant (Γ) and comparison with measured values. Data acquisition was performed at a range of about 20 m using a smart phone and a PC (master port) either via direct connection or wirelessly. Fig. 1 shows the experimental setup used to measure the RRSM properties. The method used for the evaluation of the RRSM properties in this work follows that of the self-designed system. This method is based on a comparison of the number of total counts obtained by the direct and wireless methods.

Table 1.
Commercial sensors under Study.

Sensor	SiPM	PMT	APD	PIN
Voltage supply	Low	High	Medium	Low
Size	Small	Big	Small	Small
Gain	High	High	Low	Low
Sensitivity to microphonics	No	No	Medium	Yes
Sensitivity to magnetic fields	No	Yes	No	No

Table 2.
Specifications of the SiPM used in this study.

Parameter	Value
Photosensitive area	3×3 mm^2
Number of pixels	900
Spectral response range	320–900 nm
Peak PDE (at 450 nm)	35%
Bias voltage	Vbr +1.4 V
Breakdown voltage	65 ± 10 V
Gain	2.8×10^6
Operating temperature	$-20 \sim 40$ °C

2.1. Detector design

Fig. 2 shows the detector head of the designed system. The MPPC was coupled to a CsI:Tl scintillator covered with five layers of a white diffusive (Teflon) reflector to optimize the scintillation light collection. The optical coupling was obtained by using optical grease (n=1.465) as the coupling medium (Otte et al., 2005). The coupled sensor was then covered and sealed using opaque masking tape and enclosed in an aluminum case to prevent the influence of external light and electric noise. In the experiments, we placed the radioactive sources 1 cm above the crystal without collimation (Park and Joo, 2015).

2.2. Electronic design

The electronic system shown in Fig. 3 consists of an operating circuit board mounted on a Hamamatsu S12572-100C MPPC, a power supplies board, a main circuit board, firmware for the microcontroller, an LCD display, and a Bluetooth serial interface module. The power supply board is made up of six stages designed to operate the detector, namely, 72 ± 1 VDC, amplifier ± 5 VDC, comparator +5 VDC, display device +5 VDC, microcontroller unit (MCU) board +3.3 VDC, and Bluetooth module +3.3 VDC. The detector assemblies are connected to a high-voltage subsystem. The output voltage of the high-voltage subsystem is precisely programmable (with a range of up to about 100 VDC) through a small high voltage module from UltraVolt, Inc. This system is powered by a rechargeable Li-poly battery (7.4 V, 850 mAh) (McGregor et al., 2007).

The components of the main circuit board have been optimized to run with a detector based on SiPM. The main circuit board is made up of four stages. The first stage is the operating circuit for driving the SiPM, the second is the preamplifier, which reduces the effects of noise and interference, the third is the amplifier with

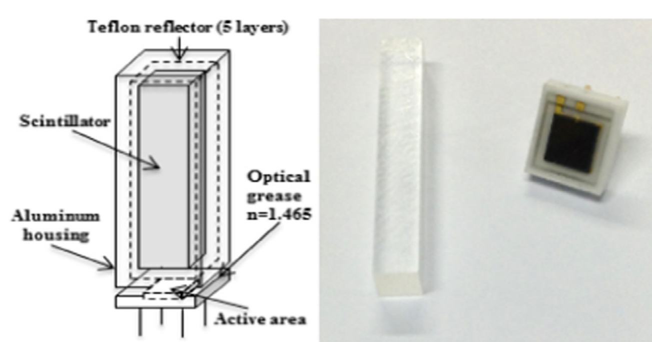

Fig. 2. Structure of the $3 \times 3 \times 20$ mm^3 CsI:Tl detector (left) together with the 3×3 mm^2 Hamamatsu S12572-100C MPPC (right).

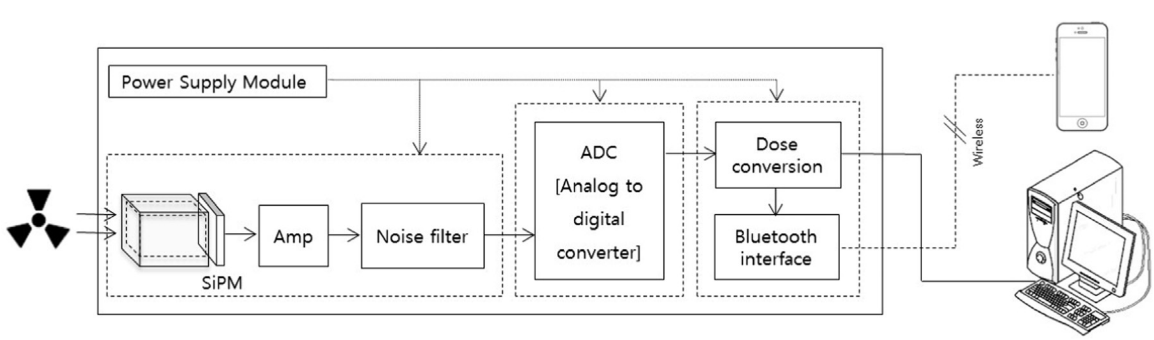

Fig. 1. Schematic of the experimental setup used for data acquisition, transfer, and processing in the RRSM system.